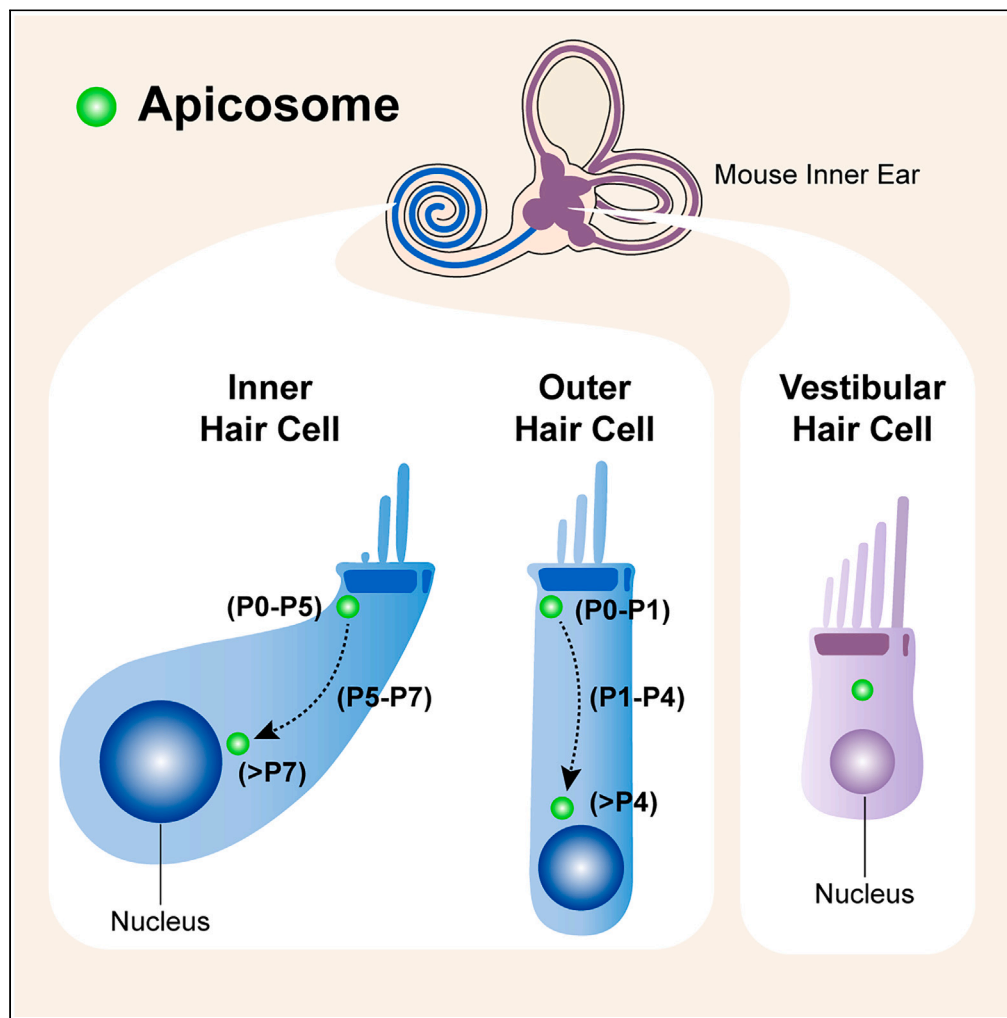**Article**

Apicosome: Newly identified cell-type-specific organelle in mouse cochlear and vestibular hair cells

Xiaofen Li, Qirui Zhao, Xiaojie Yu, ..., David Z. He, Robert Z. Qi, Pingbo Huang

bohuangp@ust.hk

Highlights

A hair-cell-specific organelle "apicosome" is identified in mouse inner ear

Apicosome exhibits itinerant nature and transient appearance in cochlear hair cells

Apicosome persists in vestibular hair cells even in adult

Apicosome is potentially associated with kinocilium maintenance and lateral inhibition

Article

Apicosome: Newly identified cell-type-specific organelle in mouse cochlear and vestibular hair cells

Xiaofen Li,[1,2,8] Qirui Zhao,[1] Xiaojie Yu,[1] Wenhan Cao,[9,10,11] Yingyi Zhang,[6,7] Wanying Feng,[1] Liwen Jiang,[9] David Z. He,[12] Robert Z. Qi,[1,13] and Pingbo Huang[1,2,3,4,5,14,*]

SUMMARY

Cochlear and vestibular hair cells are highly specialized sensory receptors for hearing and balance. Here, we report a serendipitous identification of a hair-cell-specific organelle in neonatal mouse inner ear, which we name "apicosome." The apicosome is ∼500 nm in diameter and shows itinerant nature and transient appearance during development in cochlear hair cells. In contrast to cochlear hair cells, the apicosome persists in vestibular hair cells even in adult. The timing of apicosome translocation and disappearance in cochlear hair cells during development is correlated with kinocilium development and maintenance. The apicosome is not seen in supporting cells despite the fact that nascent supporting cells have microvilli and a primary cilium. Interestingly, transdifferentiated hair cells from supporting cells also contain apicosome, suggesting that it is unique to hair cells. Thus, our study identifies a previously undescribed organelle in hair cells and lays the foundation for further characterization of this specialized structure.

INTRODUCTION

A cellular organelle is a specialized subunit responsible for a distinct function in the cell. Organelles can be either membrane-bound, such as the nucleus and mitochondrion, or non-membranous, such as the ribosome and centrosome. Whereas several organelles are present in most cell types, other organelles are highly specific to certain cell types, such as synaptic vesicles in neurons, melanosomes in melanocytes, Weibel-Palade bodies in endothelial cells, and chloroplasts in plant and algal cells. These cell-type-specific organelles are formed to serve cell-specific biological functions.

Sensory hair cells in the inner ear of vertebrates, including cochlear and vestibular hair cells, also harbor cell-specific organelles and structures required for performing their highly specialized functions—to detect sound waves and acceleration of body movements. For instance, the stereociliary bundle, which is composed of actin-based cilia (ranging in number from tens to over one hundred) displaying a staircase arrangement, is a sensory organelle through which mechanical stimuli are detected by the hair-cell transduction machinery—the mechanotransduction (MT) complex. Another example is the microtubule-based kinocilium present in vestibular hair cells and immature cochlear hair cells, but not in adult mammalian cochlear hair cells; the kinocilium inserts into the cell body at the fonticulus located at the abneural side of postnatal hair cells and is associated with the basal body. The kinocilium is considered as the specialized primary cilium of hair cell. In this sense, it is not cell-type-unique as cochlear supporting cells also have primary cilia (Figure S1). Other hair-cell-specific organelles and structures include the cuticular plate, synaptic ribbon, striated organelle (SO, or the Friedmann body),[1] and Hensen's body (HB).[2,3]

Here, we report the discovery of an organelle specific to cochlear and vestibular hair cells. We coined the term "apicosome" for this previously undescribed organelle, which exhibits a distinctive shape, size, translocation dynamics, and developmental profile. We also discuss and suggest here the potential function of the apicosome. Our work lays the foundation for further characterization of the apicosome, an organelle potentially linked to hair-cell development and morphogenesis.

RESULTS

Identification of a hair-cell-specific organelle "apicosome" in mouse inner ear

When WT mouse cochleae were fixed with PFA and immunostained with an antibody against FLRT1 (ab97825, Abcam), the signal appeared predominantly as a single distinct, large spot in the peri-cuticular

[1]Division of Life Science, Hong Kong University of Science and Technology, Hong Kong 999077, China

[2]Department of Chemical and Biological Engineering, Hong Kong University of Science and Technology, Hong Kong 999077, China

[3]State Key Laboratory of Molecular Neuroscience, Hong Kong University of Science and Technology, Hong Kong 999077, China

[4]HKUST Shenzhen Research Institute, Hong Kong University of Science and Technology, Hong Kong 999077, China

[5]Hong Kong Branch of Guangdong Southern Marine Science and Engineering Laboratory (Guangzhou), Hong Kong University of Science and Technology, Hong Kong 999077, China

[6]Biological Cryo-EM Center, Hong Kong University of Science and Technology, Hong Kong 999077, China

[7]Office of the Vice-President for Research and Development, Hong Kong University of Science and Technology, Hong Kong 999077, China

[8]Shenzhen-Hong Kong Institute of Brain Science, Shenzhen Institute of Advanced Technology, Chinese Academy of Sciences, Shenzhen 518055, China

[9]School of Life Sciences, Centre for Cell & Developmental Biology and State Key Laboratory of Agrobiotechnology, The Chinese University of Hong Kong, Shatin, New Territories, Hong Kong 999077, China

[10]State Key Laboratory of Subtropical Silviculture, Zhejiang A&F University, Hangzhou 311300, China

Continued

necklace at the neural (modiolar) side of each inner hair cell (IHC) and outer hair cell (OHC) at P0 (Figure 1A, upper panels), and the spot showed a clearly planar and apicobasal polarized distribution. The spots detected in different hair cells were mostly uniform in size (Video S1), and the apparent size variation in Figure 1A probably reflects the variation in the longitudinal positions. In control experiments, the second antibody (Alexa Fluor 488-conjugated goat anti-rabbit IgG) per se did not recognize the structure (Figure S6C). We coined the term "apicosome" to describe this newly identified structure because it initially localized in the subapical region of hair cells (see discussion); the structure is hereafter referred to as the apicosome.

Interestingly, the antigen recognized by anti-FLRT1 in apicosomes is not FLRT1: the apicosome was also recognized by anti-FLRT1 in the hair cells of *Flrt1*$^{-/-}$ mice (Figure 1A, lower panels). Our immunostaining and immunoblotting results confirmed the specificity of the anti-FLRT1 antibody (ab97825, Abcam). The antibody staining closely colocalized with the HA-staining signal of FLRT1-HA expressed in cells (Figure S2A), but the antibody weakly detected FLRT1 in western blotting and detected a strong nonspecific band of similar size (Figure S2B). In another set of experiments, a different anti-FLRT1 antibody (ab103839, Abcam) (Figure S2B) also detected the apicosome in WT hair cells, although the signal intensity was weaker (Figure 1D). The antigens used for generating the two antibodies are aa 63-253 (ab97825) and aa 50-150 (ab103839) of FLRT1, both of which are in the extracellular leucine-rich repeats of the protein. Our results suggest that the apicosome might contain a protein harboring a sequence similar to those of the two antigens, particularly the overlapping sequence: aa 63-150 of FLRT1 (see discussion).

The apicosome was also detected in P5 WT utricular hair cells (Figures 1B and 1C), as well as hair cells of P3 and P50 horizontal semicircular canal (HSC) (Figure S3) beneath the apical surface, and the size and localization of the apicosome were highly consistent in all cochlear and vestibular hair cells. By contrast, the apicosome was not seen in the surrounding supporting cells or other epithelial cells (Figures 1 and S3). These results indicate that the apicosome is a cochlear and vestibular hair-cell-specific organelle.

Next, to examine whether the apicosome is a microtubule-associated organelle, we used methanol instead of PFA to fix cochleae; this is because microtubules are fixed well by methanol, which denatures proteins but enables superior epitope exposure, whereas PFA generally preserves native structures. Interestingly, when cochleae were fixed with methanol, the apicosome appeared as a ring-shaped structure with an apparent diameter of ~500 nm rather than as a concrete spot (Figures 2A-2C). These results suggest that the apicosome is a membrane-bound organelle and further that it might be associated with microtubules because the ring-like shape is detected when microtubule integrity is preserved. To observe the precise structure of the apicosome, we conducted transmission electron microscopy (TEM) with or without immunogold labeling on cochleae from P2 WT mice. In the non-labeled specimen, a round-shaped organelle clearly located at the neuronal side of subcuticular region in the hair cell, which can be easily distinguished from mitochondria or other conventional organelles around it (Figure 2D). With FLRT1 immunogold labeling, the edge of this organelle was bound by the immunogold particles (Figure 2E), indicating that the round-shaped structure is the apicosome that we identified in immunofluorescence experiments. The size and localization of the apicosome observed by TEM were consistent with those observed by confocal microscopy after immunofluorescence labeling. Thus, as verified by TEM, the apicosome is comparable in size (diameter) to other organelles such as mitochondria (0.5-1 μm), lysosomes (0.1-1.1 μm), and melanosomes (0.5 μm).

The annulus observed here is reminiscent of what has been reported for recycling endosome clusters or vesicles surrounding centrosomes or non-centrosomal microtubule-organizing centers (ncMTOCs).[4] In hair cells, the centrosome transforms into the basal body, which controls the formation and relocation of the kinocilium,[5] but the basal body localizes at the fonticulus in postnatal hair cells, i.e., on the opposite side of the apicosome. We first suspected that the apicosome might be an organelle resembling the centrosome because (1) the apicosome appears as a single entity (or occasionally as two entities) in each hair cell; and (2) the centrosome is occasionally observed at the neural side of hair cells instead of at the opposite side like the basal body.[6] However, the apicosome did not colocalize with various centrosomal markers, such as centrin (Figure 2C), γ-tubulin, ODF2, pericentrin, and GCP6 (not shown), which suggests that the apicosome represents either a group of vesicles or a microtubule-based organelle surrounding the ncMTOC that does not contain γ-tubulin.[7] Second, the apicosome did not show staining for markers of other subcellular organelles such as the Golgi apparatus (Glogin97), mitochondria (Tom20), and early/late endosomes (Rab5/7/11) (not shown). Third, the apicosome is not the HB, a specialized

[11]Provincial Key Laboratory of Forest Aromatic Plants-based Healthcare Functions, Zhejiang A & F University, Hangzhou 311300, China

[12]Department of Biomedical Sciences, Creighton University School of Medicine, Omaha, NE 68178, USA

[13]Bioscience and Biomedical Engineering Thrust, Hong Kong University of Science and Technology (Guangzhou), Guangzhou 511453, China

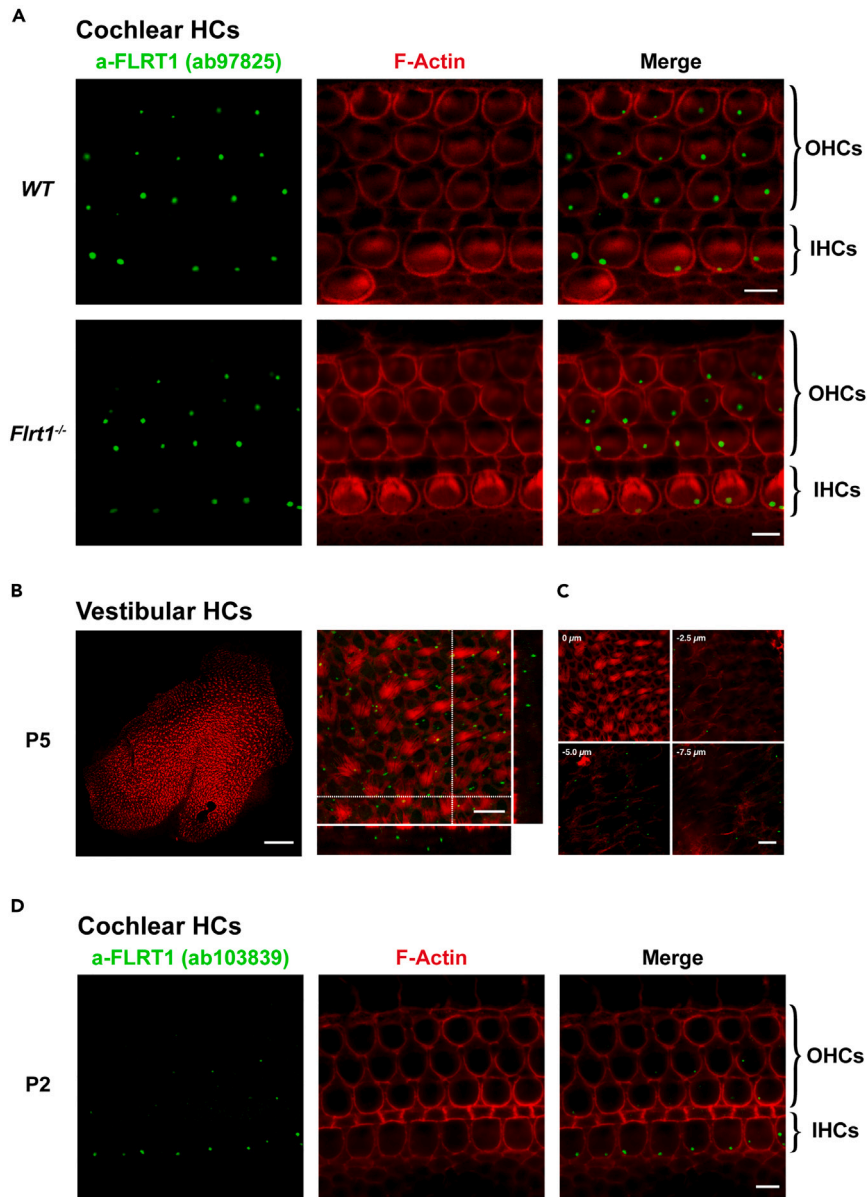[14]Lead contact

*Correspondence: bohuangp@ust.hk

Figure 1. Hair-cell-specific spot-like structure recognized by anti-FLRT1 antibodies

(A) A cochlear hair-cell-specific structure, the apicosome, was recognized by an anti-FLRT1 antibody (ab97825, Abcam) in cochlear whole mounts from P0 WT (upper) and P1 $Flrt1^{-/-}$ (lower) mice; the structure was absent in surrounding supporting cells.

(B) The apicosome was also detected in utricular hair cells from P5 WT mice. Because the apical plane of vestibular cells is not even and the hair bundles are long and floppy, the image (right) was composed of stacks of images acquired in the same area of the tissue but at distinct focal planes within a depth of ∼10 μm in order to concurrently display the apicosome and the hair bundle in multiple hair cells. The left panel is the utricular hair cells in low magnification. Dashed lines in the right panel indicate the positions of the X-Z section at bottom and Y-Z section at right.

(C) Representative images for generating the stacked image of right panel in (B), labeled with their relative Z positions.

(D) The apicosome was also recognized (albeit weakly) by a different anti-FLRT1 antibody (ab103839, Abcam) in cochlear hair cells from P2 WT mice. Phalloidin staining shows F-actin (red). Scale bars: 5 μm (A, D), 100 μm (B, left panel), and 10 μm (B, right panel and C).
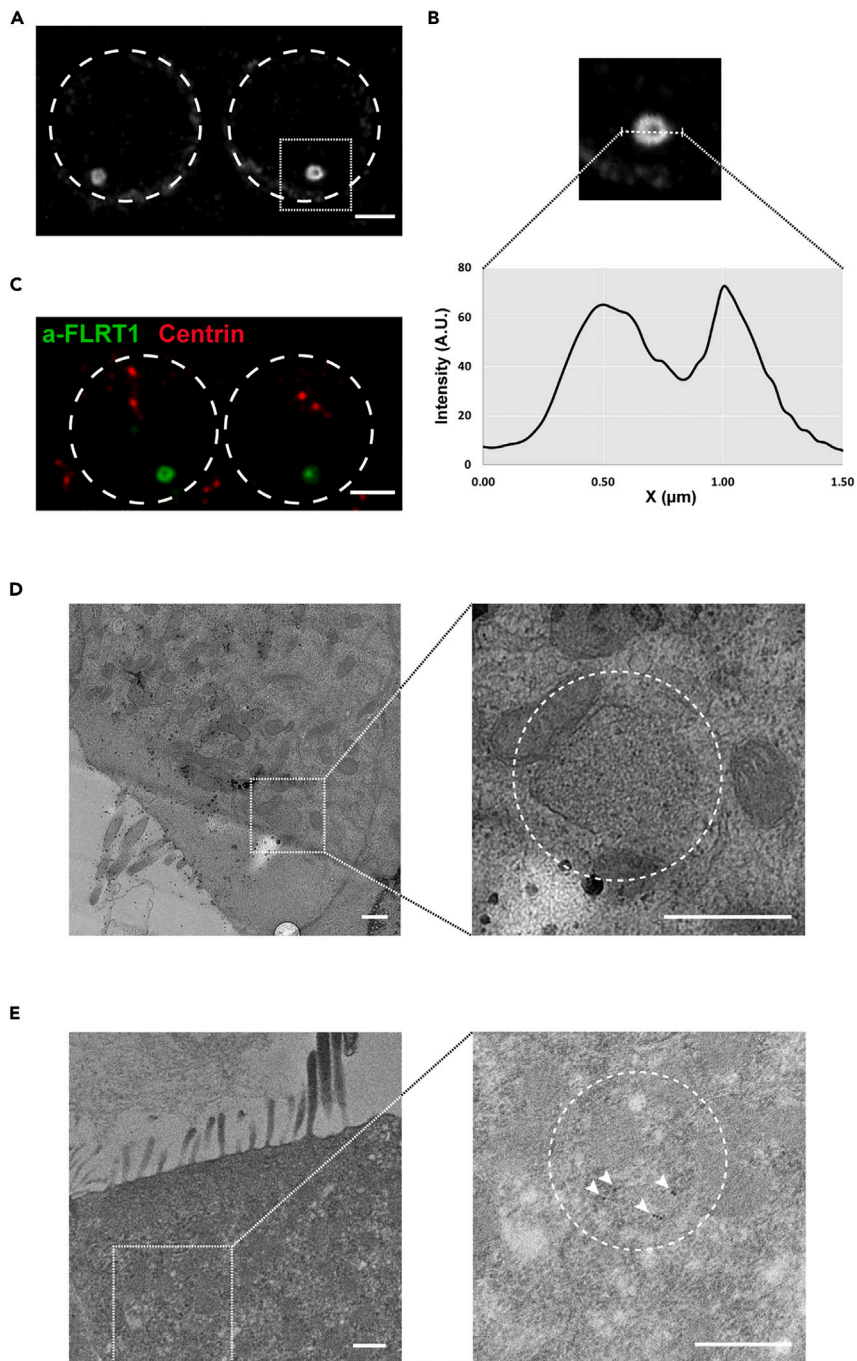
Figure 2. Apicosomes display a ring-like pattern with a diameter of ~500 nm observed by confocal microscopy after methanol fixation and TEM

The annulus of the apicosome is shown (A) as a top view in P5 IHCs and (C) in P0 IHCs with co-staining for centrin (red). (B) Image: magnification of dotted box in (A); graph: fluorescence-intensity profile of the apicosome over the 1.5-μm-long dotted line; the distance of the two fluorescence-intensity peaks from the apicosome edge gives an estimation of the apicosome diameter (~500 nm); A.U., arbitrary unit. In (C), the apicosome in the hair cell on the right is slightly out of focus, and centrin labeling in supporting cells is also visible. A round-shaped organelle with a diameter of ~500 nm can be identified without (D) and with (E) FLRT1 immunogold labeling by TEM. Right panels in (D) and (E): magnifications of the dotted boxes in left panels. Dashed circles in (A) and (C): hair-cell boundaries. Dashed circles in right panel of (D) and (E): apicosomes. Arrowheads in (E, right panel): immunogold particles. Scale bars: 2 μm (A, C) and 500 nm (D, E).
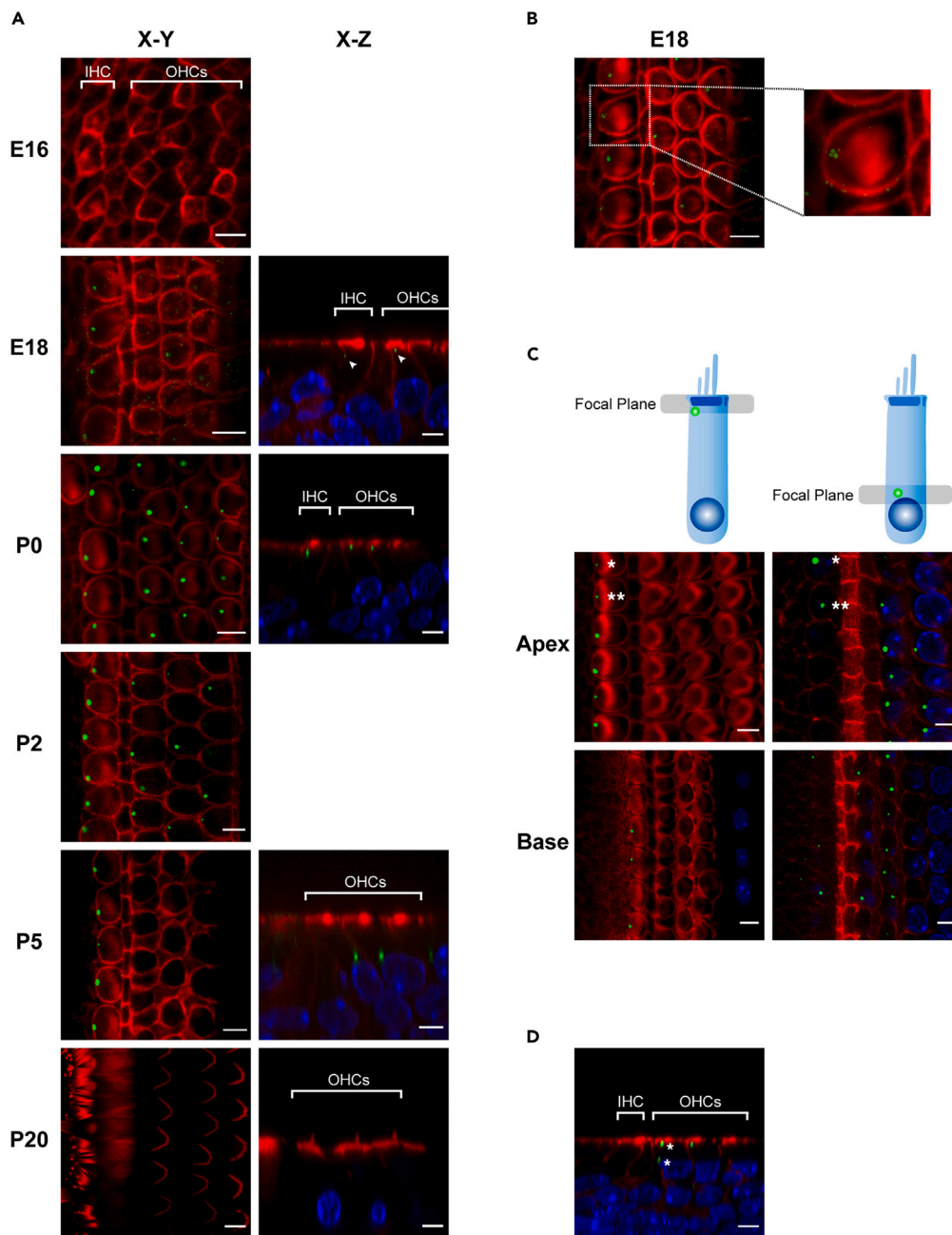
Figure 3. Apicosome developmental profile observed after PFA fixation

(A) X-Y scans of cochlear hair cells from WT mice at indicated ages (left column); some of their X-Z planes (right column) are also shown. Arrowheads: small particles or vesicles (presumably formed during apicosome assembly) detected in X-Z scans in both IHCs and OHCs at E18.

(B) X-Y scan of E18 cochlear hair cells (left) and a magnification of one IHC (right). The apicosome (right), presumably still undergoing assembly, appears as a cluster of small particles or vesicles instead of as the single spot detected in more mature hair cells. The small particles also appear to surround cortical actin, presumably at the lateral cell surface.

(C) Apicosome distribution in apical and basal turns of the cochlea from P5 WT mice. In upper schematic, gray bars indicate focal planes of images in lower panels, and positions of green dots represent typical locations of apicosomes at subapical or perinuclear regions. Panels in same row: images obtained at different focal planes from the same area; asterisks: appearance of 2 apicosomes at distinct focal planes in same cell.

Figure 3. *Continued*

(D) X-Z scan of hair cells from P0 WT mouse. Asterisks: concurrent appearance of 2 apicosomes at subapical and perinuclear positions in the same OHC. All panels: green, anti-FLRT1; red, phalloidin staining of F-actin; blue, DAPI staining of nucleus. Scale bars: 5 μm.

See also Figure S4.

structure of the ER membrane and mitochondria, because (1) the HB contains mitochondria, but the apicosome does not show staining for the mitochondrial marker Tom20; (2) the HB localizes below the fonticulus, on the side opposite to the apicosome; (3) the HB is only present in OHCs, whereas the apicosome is present in both OHCs and IHCs; and (4) the HB is considerably larger than the apicosome, ~3 μm in diameter.[2,3] Because methanol fixation denatures F-actin (and other proteins) and weakens the phalloidin staining that marks the hair-cell boundary, we used PFA fixation in subsequent experiments for clear visualization of the hair-cell boundary and apicosome itself.

Developmental profile of apicosome in hair cells

We next examined the developmental profile of the apicosome in cochlear hair cells. No apicosome signal was detected in embryonic day (E) 16 hair cells (Figure 3A), but by around E18, the apicosome was observed as a cluster of small particles or vesicles at the neural side of the peri-cuticular necklace (Figures 3A and 3B); this presumably reflects the initial assembly of the apicosome. Notably, between P0 and P4, the apicosome descended from the peri-cuticular necklace to the perinuclear region of OHCs (Figures 3A and S4). This timing of apicosome translocation depended on the cell type and tonotopic gradient. First, the translocation occurred earlier in OHCs than IHCs within the same region of the organ of Corti: the apicosome descended in most OHCs by P5 but remained subapical in nearly all IHCs at this stage (Figure 3A); the apicosome descended to the perinuclear region and became dispersed in all hair cells only after P7 (Figure 3A). Second, the apicosome remained subapical in all the IHCs in the apex of the cochlea at P5 but showed subapical localization in <50% of the IHCs in the cochlear base (Figure 3C); this suggests that apicosome translocation occurs earlier at the basal than apical turns of the cochlea. By contrast, the apicosome persisted in adult (P50) HSC hair cells (Figure S3B), although it became smaller and more distant from the apical membrane compared to that in neonatal vestibular cells (Figure S3). Because kinocilia disappear after P10 in cochlear hair cells and persist in neonatal and adult vestibular cells, similar to the expression of the apicosome in cochlear and vestibular hair cells, we speculate that the presence of the apicosome is associated with kinocilium maintenance. In addition, kinocilia in OHCs appear to be resorbed earlier than those in IHC in mice and gerbils,[8,9] consistent with the timing of apicosome translocation and disappearance.

Interestingly, in a few hair cells, the apicosome was split and appeared concurrently at the subapical and perinuclear positions (Figures 3C and 3D; Video S1). By contrast, in most hair cells, the apicosome was found at either the subapical position or the perinuclear position as an entire entity and was seldom detected between the two positions (Figure 3A). Thus, the apicosome might move from the apical position to the perinuclear position presumably in small steps, similar to the initial assembly (Figures 3A and 3B), but this might occur too rapidly to be recorded in most hair cells. Alternatively, the apicosome might translocate as a single entity.

Potential association of apicosome with lateral inhibition

Sporadically, supernumerary IHCs was observed in the cochlea in WT mice (Figure 4A and 1A); this might reflect minor fluctuations or errors in the control system of lateral inhibition during normal hair-cell development[10]. The apicosome in these regions exhibited atypical features: (1) some of the hair cells contained more than one apicosome, and (2) the position of the apicosome was considerably outside its normal position (Figure 4A). Thus, the abnormal appearance of the apicosome appears to be potentially associated with lateral inhibition. To further test this idea, we treated cochlear organ cultures with the γ-secretase inhibitor DAPT to disrupt Notch signaling pathway/lateral inhibition and generate supernumerary hair cell-like cells from *trans*-differentiation of supporting cells. Notably, the apicosome appeared in the supernumerary hair cells that are converted from supporting cells, further strengthening the notion that the apicosome is linked with hair-cell specification and differentiation (Figures 4B and 4C). Moreover, the apicosome in the DAPT-induced supernumerary hair cells also show abnormal features similar to those in Figure 4A (Figures 4B and 4C), and these results bolster the association of atypical apicosome appearance with
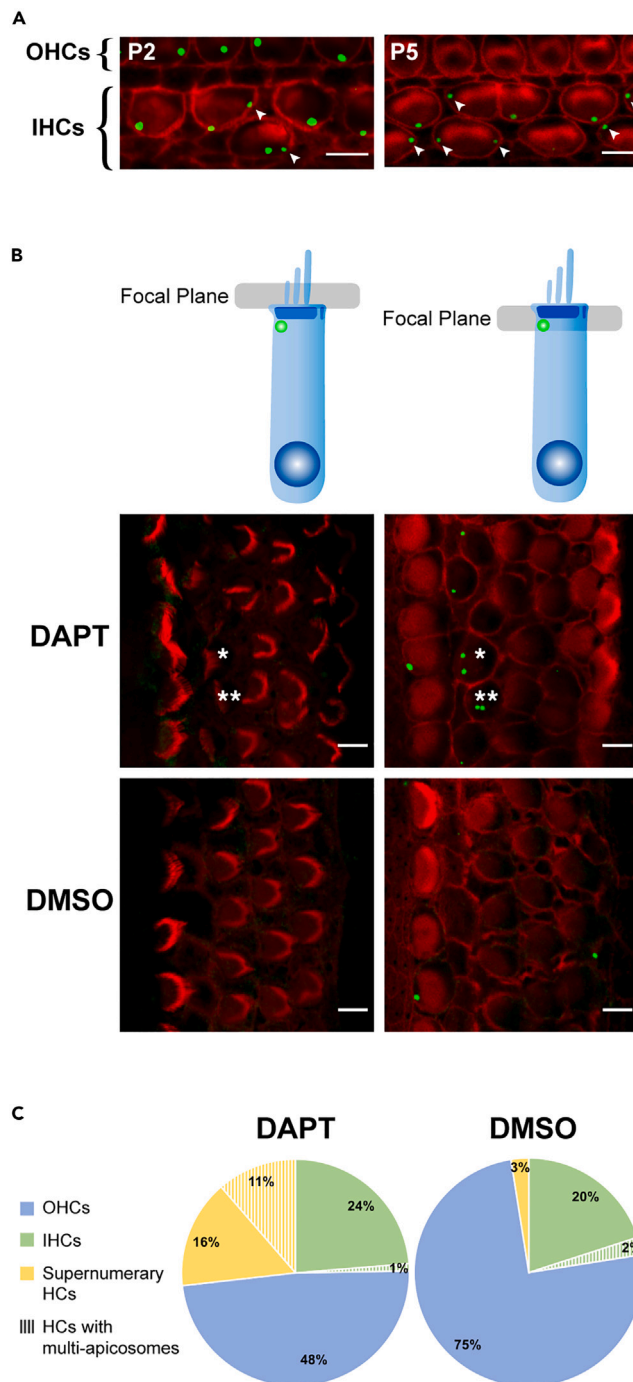
Figure 4. Apicosome localization and number in supernumerary HCs

(A) Apicosomes in supernumerary IHCs from P2 (left) and P5 (right) WT mice. Arrowheads: apicosomes exhibiting atypical localization—not at the neural side of hair cells. Scale bars: 5 μm.

(B) Atypical localization of the apicosome is also seen in supernumerary HCs (P0 + 5 DIV) induced by DAPT treatment in apical-middle turns of WT cochlear cultures. The apicosomes already translocate and are not seen in the focal planes of these images in most of the cells. Asterisks: the same cell at different focal planes. Green: anti-FLRT1; red: phalloidin staining of F-actin. Scale bars: 5 μm.

(C) Percentages of supernumerary HCs and HCs with multi-apicosomes both increase in cochlear cultures upon DAPT treatment. In total, 40 HCs in the apical region of DMSO (vehicle) treated samples and 97 of DAPT treated samples were counted.
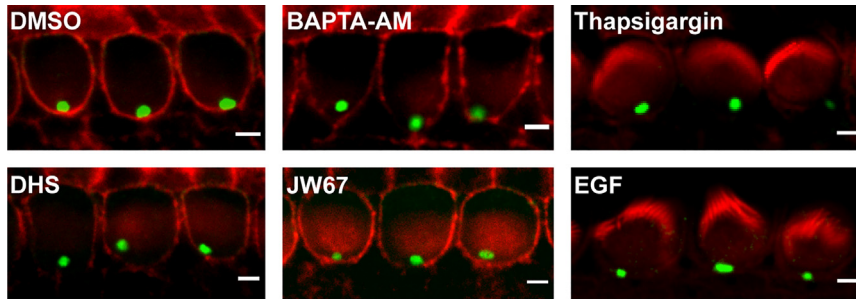
Figure 5. Apicosomes remain stable under various treatments
Apicosomes and F-actin were stained with anti-FLRT1 (green) and phalloidin (red), respectively, in P2+1DIV IHCs after treatment with indicated reagents for 6 h at 37°C. DMSO, solvent control. Scale bars: 2 μm.

abnormal lateral inhibition. However, the apicosome did not appear to contain Delta-like ligand1 (DLL1) of Notch receptors, based on our immunostaining study with an antibody against DLL1 (not shown).

Lastly, to gain additional insights into the biological nature of the apicosome, we examined whether the apicosome was affected when cochlear cultures were exposed to various reagents; we treated P2+1 DIV organ of Corti cultures for 6 h with following reagents: BAPTA-AM or thapsigargin, for reducing or increasing intracellular Ca^{2+} levels; DHS, for blocking the MT channel (and hair-cell maturation); JW67, for inhibiting Wnt signaling; and EGF. However, the apicosome showed no change after each treatment and remained at the peri-cuticular necklace under the apical surfaces in all IHCs (Figure 5).

DISCUSSION

We identified an organelle exhibiting a unique localization, translocation, and developmental profile in both cochlear and vestibular hair cells, and have coined the name "apicosome" for this previously unde-scribed organelle. Although the apicosome was fortuitously detected based on its recognition by two anti-FLRT1 antibodies, the organelle does not contain FLRT1, because anti-FLRT1 detected the apicosome even in $Flrt1^{-/-}$ mice (Figure 1). Moreover, FLRT1 itself does not appear to be involved in any aspect of hair-cell function or development: the results of ABR assays showed that hearing function was normal in 1-month-old $Flrt1^{-/-}$ mice (Figure S5).

Could the apicosome contain the FLRT1 homologs FLRT2 and FLRT3? FLRT2 and FLRT3 share high sequence similarity with FLRT1 (61% and 71%, respectively),[11] and, more importantly, FLRT3 might be involved in hearing: an FLRT3 mutation (205C>A) was reported to be associated with hearing loss through the FGF signaling pathway.[12] However, the apicosome was not recognized by anti-FLRT2 and anti-FLRT3 antibodies (Figure S6) whose specificity was validated here (Figures S6A and S6B; data not shown for anti-FLRT3). FLRT ectodomains contain metalloprotease cleavage sites and can be shed from FLRT-expressing cells[13]; thus, we reasoned that blocking the cleavage of the ectodomains of cell-surface FLRTs might alter apicosome size or dynamics if the apicosome acts as an intracellular pool of FLRTs. However, 10-h treatment of organ of Corti cultures (P0+2 DIV) with metalloprotease inhibitors (20 μg/mL TAPI-0 and TAPI-1) did not affect apicosome localization or dynamics (not shown). To further identify candidate target proteins recognized by anti-FLRT1 in the apicosome, we performed BLAST searches by using the FLRT1 sequences aa 63-253, 50-150, and 63-150, the antigens of the two anti-FLRT1 antibodies (ab97825 and ab103839) and their overlapping region. However, all the BLAST searches yielded only FLRT1 proteins from various species. One possibility is that the two anti-FLRT1 antibodies recognize a secondary or tertiary structure rather than a primary sequence in the apicosome. Thus, mass spectrometry analysis of proteins immunoprecipitated using the anti-FLRT1 antibodies might represent an effective approach for addressing this matter. A precedent here can be found in the identification of PCDH15: in the tip link of hair cells, PCDH15 was first detected by an unidentified antibody, and the molecular identity of PCDH15 was only revealed later by using mass spectrometry.[14]

The translocation trajectory of the apicosome before complete disappearance was found to be highly characteristic and consistent—from the subapical location at the neural side to the perinuclear position. This is reminiscent of the translocation of certain latent gene regulatory proteins such as Notch, β-catenin, and

Smads; these molecules traffic from the cell surface or the cytoplasm into the nucleus and function in lateral inhibition, planar cell polarity signaling, or pattern formation. However, these signaling molecules are all translocated as soluble proteins and require no membranous vesicle such as the apicosome. Interestingly, apicosome translocation itself might be mediated by microtubules, because our results (Figure 2) suggested that the apicosome represents either a group of vesicles or a microtubule-based ncMTOC-surrounding organelle lacking γ-tubulin. Microtubules are known to be present throughout the cell body in both OHCs and IHCs, and some of these microtubules are concentrated in the tubulo-vesicular track[15] and could therefore serve as the track for apicosome translocation. Another potential track is the SO. Although the precise composition of the SO is unclear, it contains α2-spectrin, and the SO is also present throughout the cell body.[6] However, the SO is present in vestibular and cochlear IHCs but not OHCs,[6] whereas the apicosome is present in both IHCs and OHCs.

In summary, we serendipitously identified a previously unrecognized hair-cell-specific organelle, the apicosome; the organelle shows a distinctive localization, translocation, and developmental profile and is potentially associated with kinocilium maintenance and lateral inhibition. The itinerant nature and transient appearance of the apicosome during development might explain why the organelle remained unnoticed over the past several decades of research on hair cells. The critical question to address next is the molecular composition of the apicosome, including the protein recognized by anti-FLRT1; this will be essential for elucidating the function, regulation, and translocation of the apicosome. Nevertheless, our work lays the foundation for further characterization of this unique structure potentially linked to hair-cell development and function.

Limitations of study

Although we have clearly demonstrated the presence of the apicosome in hair cells with immunocytochemical and electron-microscopic techniques, the exact molecular compositions of this newly described organelle remain unclear.

STAR★METHODS

Detailed methods are provided in the online version of this paper and include the following:

- KEY RESOURCES TABLE
- RESOURCE AVAILABILITY
  - Lead contact
  - Materials availability
  - Data and code availability
- EXPERIMENTAL MODEL AND SUBJECT DETAILS
  - Animals
  - Cell lines
- METHOD DETAILS
  - Genotyping
  - Cochlear culture and treatments
  - Transfection
  - Immunohistochemical assays
  - Transmission electron microscopy (TEM) and immunogold labeling
  - Auditory brainstem response (ABR)
- QUANTIFICATION AND STATISTICAL ANALYSIS

SUPPLEMENTAL INFORMATION

Supplemental information can be found online at https://doi.org/10.1016/j.isci.2023.106535.

REFERENCES

1. Pollock, L.M., and McDermott, B.M., Jr. (2015). The cuticular plate: a riddle, wrapped in a mystery, inside a hair cell. Birth Defects Res. C Embryo Today. *105*, 126–139. https://doi.org/10.1002/bdrc.21098.

2. Lim, D.J. (1986). Functional structure of the organ of Corti: a review. Hear. Res. *22*, 117–146. https://doi.org/10.1016/0378-5955(86)90089-4.

3. Mammano, F., Frolenkov, G.I., Lagostena, L., Belyantseva, I.A., Kurc, M., Dodane, V., Colavita, A., and Kachar, B. (1999). ATP-Induced Ca2+ release in cochlear outer hair cells: localization of an inositol triphosphate-gated Ca2+ store to the base of the sensory hair bundle. J. Neurosci. *19*, 6918–6929. https://doi.org/10.1523/jneurosci.19-16-06918.1999.

4. Sanchez, A.D., and Feldman, J.L. (2017). Microtubule-organizing centers: from the centrosome to non-centrosomal sites. Curr. Opin. Cell Biol. *44*, 93–101. https://doi.org/10.1016/j.ceb.2016.09.003.

5. Sienknecht, U.J. (2015). Current concepts of hair cell differentiation and planar cell polarity in inner ear sensory organs. Cell Tissue Res. *361*, 25–32. https://doi.org/10.1007/s00441-015-2200-1.

6. Vranceanu, F., Perkins, G.A., Terada, M., Chidavaenzi, R.L., Ellisman, M.H., and Lysakowski, A. (2012). Striated organelle, a cytoskeletal structure positioned to modulate hair-cell transduction. Proc. Natl. Acad. Sci. USA *109*, 4473–4478. https://doi.org/10.1073/pnas.1101003109.

7. Zheng, Y., Buchwalter, R.A., Zheng, C., Wight, E.M., Chen, J.V., and Megraw, T.L. (2020). A perinuclear microtubule-organizing centre controls nuclear positioning and basement membrane secretion. Nat. Cell Biol. *22*, 297–309. https://doi.org/10.1038/s41556-020-0470-7.

8. Lim, D.J., and Anniko, M. (1985). Developmental morphology of the mouse inner ear: a scanning electron microscopic observation. Acta Otolaryngol. *99*, 5–69. https://doi.org/10.3109/00016488509121766.

9. Jia, S., Yang, S., Guo, W., and He, D.Z.Z. (2009). Fate of mammalian cochlear hair cells and stereocilia after loss of the stereocilia. J. Neurosci. *29*, 15277–15285. https://doi.org/10.1523/JNEUROSCI.3231-09.2009.

10. Verpy, E., Leibovici, M., Michalski, N., Goodyear, R.J., Houdon, C., Weil, D., Richardson, G.P., and Petit, C. (2011). Stereocilin connects outer hair cell stereocilia to one another and to the tectorial membrane. J. Comp. Neurol. *519*, 194–210. https://doi.org/10.1002/cne.22509.

11. Lacy, S.E., Bönnemann, C.G., Buzney, E.A., and Kunkel, L.M. (1999). Identification of FLRT1, FLRT2, and FLRT3: a novel family of transmembrane leucine-rich repeat proteins. Genomics *62*, 417–426. https://doi.org/10.1006/geno.1999.6033.

12. Miraoui, H., Dwyer, A.A., Sykiotis, G.P., Plummer, L., Chung, W., Feng, B., Beenken, A., Clarke, J., Pers, T.H., Dworzynski, P., et al. (2013). Mutations in FGF17, IL17RD, DUSP6, SPRY4, and FLRT3 are identified in individuals with congenital hypogonadotropic hypogonadism. Am. J. Hum. Genet. *92*, 725–743. https://doi.org/10.1016/j.ajhg.2013.04.008.

13. Yamagishi, S., Hampel, F., Hata, K., Del Toro, D., Schwark, M., Kvachnina, E., Bastmeyer, M., Yamashita, T., Tarabykin, V., Klein, R., and Egea, J. (2011). FLRT2 and FLRT3 act as repulsive guidance cues for Unc5-positive neurons. EMBO J. *30*, 2920–2933. https://doi.org/10.1038/emboj.2011.189.

14. Ahmed, Z.M., Goodyear, R., Riazuddin, S., Lagziel, A., Legan, P.K., Behra, M., Burgess, S.M., Lilley, K.S., Wilcox, E.R., Riazuddin, S., et al. (2006). The tip-link antigen, a protein associated with the transduction complex of sensory hair cells, is Protocadherin-15. J. Neurosci. *26*, 7022–7034. https://doi.org/10.1523/JNEUROSCI.1163-06.2006.

15. Furness, D.N., Hackney, C.M., and Steyger, P.S. (1990). Organization of microtubules in cochlear hair cells. J. Electron. Microsc. Tech. *15*, 261–279. https://doi.org/10.1002/jemt.1060150306.

16. Xiong, W., Wagner, T., Yan, L., Grillet, N., and Müller, U. (2014). Using injectoporation to deliver genes to mechanosensory hair cells. Nat. Protoc. *9*, 2438–2449. https://doi.org/10.1038/nprot.2014.168.

17. Li, Y., Jia, S., Liu, H., Tateya, T., Guo, W., Yang, S., Beisel, K.W., and He, D.Z.Z. (2018). Characterization of hair cell-like cells converted from supporting cells after Notch inhibition in cultures of the organ of Corti from neonatal gerbils. Front. Cell. Neurosci. *12*, 73.

18. Hu, W., Yu, X., Liu, Z., Sun, Y., Chen, X., Yang, X., Li, X., Lam, W.K., Duan, Y., Cao, X., et al. (2017). The complex of TRIP-Br1 and XIAP ubiquitinates and degrades multiple adenylyl cyclase isoforms. Elife *6*, e28021. https://doi.org/10.7554/eLife.28021.

19. Li, X., Yu, X., Chen, X., Liu, Z., Wang, G., Li, C., Wong, E.Y.M., Sham, M.H., Tang, J., He, J., et al. (2019). Localization of TMC1 and LHFPL5 in auditory hair cells in neonatal and adult mice. FASEB J *33*, 6838–6851. https://doi.org/10.1096/fj.201802155RR.

STAR★METHODS

KEY RESOURCES TABLE

REAGENT or RESOURCE	SOURCE	IDENTIFIER
Antibodies		
Rabbit polyclonal anti-FLRT1	Abcam	Cat# ab97825; RRID: AB_10696255
Rabbit polyclonal anti-FLRT1	Abcam	Cat# ab103839; RRID: AB_10860459
Rabbit polyclonal anti-FLRT2	Abcam	ab154023
Mouse monoclonal anti-FLRT2	R&D Systems	Cat# MAB2877; RRID: AB_2106599
Goat polyclonal anti-FLRT3	R&D Systems	Cat# AF2795; RRID: AB_2106855
Mouse monoclonal anti-Centrin	EMD Millipore	Cat# 04-1624; RRID: AB_10563501
Mouse monoclonal anti-HA	BioLegend	Cat# 901502; RRID: AB_2565007
Alexa Fluor 488-conjugated goat anti-rabbit IgG	Thermo Fisher Scientific	Cat# A27034; RRID: AB_2536097
Alexa Fluor 488-conjugated donkey anti-goat IgG	Abcam	Cat# ab150129; RRID: AB_2687506
Alexa Fluor 647-conjugated goat anti-mouse IgG	Abcam	Cat# ab150115; RRID: AB_2687948
Biotinylated goat anti-rabbit IgG	Thermo Fisher Scientific	Cat# 65-6140; RRID: AB_2533969
TRITC-conjugated phalloidin	Sigma-Aldrich	Cat# P1951; RRID: AB_2315148
Alexa Fluor 647-conjugated phalloidin	Thermo Fisher Scientific	Cat# A22287; RRID: AB_2620155
Chemicals, peptides, and recombinant proteins		
Ampicillin sodium	Goldbio	A-301
BAPTA-AM	Sigma-Aldrich	A1076
Bovine serum albumin	Sigma-Aldrich	A2153
DAPT	Santa Cruz	CAS208255-80-5
Dihydrostreptomycin	Sigma-Aldrich	D1954000
DMEM	Gibco	12800082
DMEM/F-12	Gibco	12500-062
DMSO	Sigma-Aldrich	276855
Embed 812 resin	Electron Microscopy Sciences	14120
Epidermal growth factor	Thermo Fisher Scientific	PHG0311
FBS	Gibco	10270-106
HBSS	Gibco	14175103
JW67	Sigma-Aldrich	SML0324
Paraformaldehyde	Sigma-Aldrich	P6148
Polyethylenimine	Polysciences	23966
Pro-Long Gold Antifade Mountant with DAPI	Thermo Fisher Scientific	P36931
Thapsigargin	Sigma-Aldrich	T9033
Triton X-100	BDH	30632
Experimental models: Cell lines		
Human: HEK293T cells	ATCC	RRID:CVCL_1926
Chlorocebus aethiops: COS-7 cells	ATCC	RRID:CVCL_0224
Experimental models: Organisms/strains		
Mice: C57BL/6J	The Jackson Laboratory	RRID:IMSR_JAX:000664
Mice: B6.129S5- *Flrt1*^{tm1Lex}/Mmucd	MMRRC	RRID:MMRRC_032313-UCD
Recombinant DNA		
Plasmid: pcDNA3-Flrt1-HA	This paper	N/A

(Continued on next page)

Continued

REAGENT or RESOURCE	SOURCE	IDENTIFIER
Plasmid: pcDNA3-Flrt2-HA	This paper	N/A
Software and algorithms		
Fiji	Fiji	https://fiji.sc
Leica LAS AF/LAS X	Leica	https://www.leica-microsystems.com/products/microscope-software/p/leica-las-x-ls/
BioSigRZ	Tucker-Davis Technologies	https://www.tdt.com/component/biosigrz-abr-dpoae-software/

RESOURCE AVAILABILITY

Lead contact

Further information and requests for resources and reagents should be directed to and will be fulfilled by the lead contact, Pingbo Huang (bohuangp@ust.hk).

Materials availability

This study did not generate new unique reagents.

Data and code availability

- Data reported in this paper will be shared by the lead contact upon request.

- This paper does not report original code.

- Any additional information required to reanalyze the data reported in this paper is available from the lead contact upon request.

EXPERIMENTAL MODEL AND SUBJECT DETAILS

Animals

C57BL/6J mice (The Jackson Laboratory; RRID: IMSR_JAX:000664) were used as wild-type (WT) mice in this study. FLRT1-knockout (KO; $Flrt1^{-/-}$) mouse sperm was purchased from MMRRC (B6.129S5-$Flrt1^{tm1Lex}$/Mmucd; RRID: MMRRC_032313-UCD) to generate KO mice with the C57BL/6 background. Mice at the ages of E16-E18, P0-P50 were used in this study, as indicated in figures and methods for each experiment. Littermates of both sexes were randomly assigned to experimental groups. All animal procedures were approved by the University Committee on Research Practices at the Hong Kong University of Science and Technology (Ethics Protocol: 2018001).

Cell lines

HEK293T cells (RRID: CVCL_1926) and COS-7 cells (RRID: CVCL_0224) were obtained from American Type Culture Collection (ATCC, Manassas, VA, USA). The cells were presumably authenticated by ATCC and were not further authenticated in this study. The cell lines, which routinely tested negative for mycoplasma contamination, were maintained in DMEM supplemented with 10% (v/v) fetal bovine serum (FBS) and 100 μg/mL ampicillin in an atmosphere of 95% air and 5% CO2 at 37°C.

METHOD DETAILS

Genotyping

$Flrt1^{-/-}$ mice were genotyped using these primers: 5'-GCACCACACGAGGCTACCG-3' (sense) and 5'-ACATCTCCAACAATGCTGAATCCC-3' (antisense), designed to produce a 271-bp wild-type (WT) band; and 5'-GCAGCGCATCGCCTTCTATC-3' (sense) and the WT antisense primer, to produce a 371-bp KO band. Amplification reactions were performed using Taq DNA polymerase at 61°C annealing temperature.

Cochlear culture and treatments

Cochlear culture was performed following a published protocol.[16] Briefly, the organ of Corti was dissected from postnatal day (P) 2 WT mice, attached on the bottom of a 35-mm culture dish, and incubated in DMEM/F-12 medium containing 1% (v/v) FBS and 1.5 μg/mL ampicillin at 37°C overnight before treatment.

Cochlear cultures were treated for 6 h with various reagents (all dissolved in culture medium): 0.1% (v/v) DMSO, 0.5 mM BAPTA-AM, 1 μM thapsigargin, 0.1 mM dihydrostreptomycin (DHS), 0.1 mM JW67, or 100 ng/mL epidermal growth factor (EGF).

To block Notch signaling, DAPT, a γ-secretase inhibitor, was used as previously described.[17] The cultures prepared from P0 WT mice were treated with 5 μM DAPT or 0.05% (v/v) DMSO (vehicle) for 48 h; the cultures were then washed and incubated for additional 48 h in fresh culture media. The samples were fixed, immunostained, and imaged. Unless indicated otherwise, most of HC immunostaining images were obtained from apex or middle turns of the cochleae. At least three cochleae from distinct mice were used for each experimental condition.

Transfection

Cells were cultured and transfected according to our published procedures.[18] All transfections were performed using polyethylenimine. Cells were transiently transfected with pcDNA3-Flrt1-HA or pcDNA3-Flrt2-HA, and, after culturing for 48 h, were subject to western blotting or immunostaining.

Immunohistochemical assays

Cochlear tissues were immunostained following our published procedures.[19] Briefly, tissues were fixed with 4% (w/v) paraformaldehyde (PFA) or ice-cold methanol, immersed in HBSS containing 0.1 mM $CaCl_2$, 4% (w/v) bovine serum albumin (BSA), and 0.5% (v/v) Triton X-100 for blocking and permeabilization, and then incubated with primary antibodies (1:200 anti-FLRT1, anti-FLRT2, or anti-FLRT3) at room temperature for 4 h. Subsequently, the samples were washed thrice (10 min each) with HBSS containing 0.1 mM $CaCl_2$ and incubated with Alexa Fluor 488-conjugated second antibodies (1:200) and Alexa Fluor 647-conjugated phalloidin (1:40) at room temperature for 2 h. After washing thrice (10 min each) with HBSS containing 0.1 mM $CaCl_2$, the samples were mounted using Pro-Long Gold Antifade Mountant with DAPI.

In the case of COS-7 cells, at 48 h after transfection with FLRT1-HA or FLRT2-HA plasmids, the cells were fixed with 4% PFA for 1 h, washed once with PBS, blocked and permeabilized with PBS containing 4% BSA and 0.5% Triton X-100 for 1 h, and then incubated with primary antibodies (1:200) at room temperature for 4 h. After washing thrice (10 min each) with PBS, the cells were incubated with Alexa Fluor 488-conjugated goat anti-rabbit IgG (1:200) and Alexa Fluor 647-conjugated goat anti-mouse IgG (1:200) plus TRITC-conjugated phalloidin (1:400) at room temperature for 2 h. Lastly, the cells were washed thrice (10 min each) with PBS and mounted for examination under a confocal microscope. All confocal microscopy was performed using Leica TCS Sp5 or Leica TCS Sp8 confocal microscopes (Leica Microsystems, Buffalo Grove, IL, USA) (objectives: 10×/0.4 NA and 100×/1.4 NA for whole-mount cochleae; 63×/1.4 NA for whole-mount vestibular tissues and COS-7 cells). Leica LAS AF and LAS X imaging software and Fiji software (https://fiji.sc) were used for image acquisition and analysis.

Transmission electron microscopy (TEM) and immunogold labeling

Cochleae collected from P2 WT mice were fixed with 4% (w/v) PFA in 0.1 M sodium phosphate buffer (PB, pH 7.4) at room temperature for 2 h, and then kept at 4°C for 12 h; the cochleae were punched with small holes in apex and base areas for better perfusion. After washed thrice with 0.1 M PB, the organs of Corti were then dissected from the fixed cochleae. For post fixation, the organs of Corti were treated with 1% (w/v) osmium tetroxide (OsO_4) in 0.1 M PB for 20 min at room temperature and washed with 0.1 M PB for at least 5 times (OsO_4 fixation should be skipped if the samples were subject to immunolabeling). The organs of Corti were dehydrated in a graded series of acetone solutions (50%, 70%, 90%, 100%, and dry 100%). Then, the dehydrated organs of Corti were infiltrated in a mixture of acetone and Embed 812 resin, and polymerized in fresh pure resin at 60°C for 24 h.

The organs of Corti embedded in Embed 812 resin were sectioned with a histo-diamond knife (Diatome) on the ultramicrotome (Leica EM UC7, Leica Microsystems). Ultra-thin sections (80 nm in thickness) were made and collected on 3 mm-diameter nickel grids.

If immunolabeling was not required, the grids were only stained with 2% uranyl acetate for 10 min and 1% lead citrate for 5 min. While for immunogold labeling, grids were immersed in droplets of the following solutions sequentially within a humid chamber: tris-buffered saline (TBS) to wash once; 10% (v/v) rabbit serum and 0.2% (v/v) Tween 20 in TBS for 30 min at room temperature to block nonspecific protein binding;

anti-FLRT1 antibody (ab97825, 1:30) in 0.05 M TBS containing 1% (w/v) BSA (BSA-TBS) at 4°C overnight; 0.5% (v/v) Tween 20 in TBS (T20-TBS) for 5 times (5 min each); biotinylated goat anti-rabbit IgG (1:100) in BSA-TBS for 1.5 h at room temperature; T20-TBS twice (5 min each); BSA-TBS twice (5 min each); STP-gold (1:10) in BSA-TBS for 1 h at room temperature; T20-TBS twice (5 min each); distilled water thrice (5 min each). Grids containing sections as negative controls were incubated in BSA-TBS without the primary antibody. Then, the grids were lightly counterstained with 2% uranyl acetate for 10 min and 1% lead citrate for 2 min.

As for imaging, the EM grids were screened using Tecnai transmission electron microscope (Thermo Fisher Scientific), operated at 120 keV. Images were taken with Ceta camera with the desired calibrated magnifications at the Biological Cryo-EM Center of the Hong Kong University of Science and Technology.

Auditory brainstem response (ABR)

ABR measurements were obtained using our published procedures.[19] Briefly, 1-month-old mice were anesthetized and placed in a sound-proof chamber for test. RZ6-based TDT system III hardware and BioSigRZ software (Tucker-Davis Technologies, Alachua, FL, USA) were used for stimulus presentation and response recording. The broadband click stimuli were applied with a duration of 0.1 ms at indicated sound levels; the pure tone stimuli (8–32 kHz) were applied with a duration of 5 ms, starting at 90 dB SPL and decreasing by 10-dB steps. Auditory thresholds were determined by visual estimation.

QUANTIFICATION AND STATISTICAL ANALYSIS

All statistical data are expressed as means $\pm$ SEM. Two-tailed Student's t test was used for statistical analysis, and $p < 0.05$ was considered statistically significant.